Deep Learning Driven Automated Red Palm Weevil Detection Using Sparrow Search Optimization

Narek Badjajian[1,] *, Warshine Barry[1]

[1]University of Debrecen, Department of Mathematical and Computational Science, Debrecen, Hungary

Emails: badjajiann6math@gmail.com, warshinabarrykurd@gmail.com

Abstract

In recent decades, Red Palm Weevils (RPW) have been demonstrated as a harmful pest of palm trees worldwide, predominantly in the Middle East. The RPW is produced massive damage to several palm varieties. Primary detection of the RPW is a complex problem to optimum date production while the recognition is avoided by palm trees as to be influenced by RPW. Several studies are driven to determine a precise approach for the detection, localization, and classification of RPW pests. Employing computer vision (CV) technology with pattern detection is verified that further productive once utilized for identifying and classifying insects. Thus, the automated method decreases either the problem or labor effort required for enhancing the farmer's income. The farmers can be stimulated to enhance the productivity of date fruit once this has been done. With this motivation, this article focuses on the design of automated RPW pest detection using sparrow search optimization with deep learning (RPWPD-SSODL) technique. The presented RPWPD-SSODL algorithm mostly focused on the detection and classification of RPW using computer vision approaches. To accomplish this, the RPWPD-SSODL technique employs bilateral filtering (BF) for noise removal. Next, the RPWPD-SSODL technique uses Dense-RefineDet object detector with ShuffleNet model as a backbone network. For improving the recognition solution, the hyperparameter tuning of the ShuffleNet model can be optimally adjusted using the SSO algorithm. To validate the simulation results of the RPWPD-SSODL technique, a wide-ranging simulation outcome is implemented. The simulation values potrayed the improvement of the RPWPD-SSODL algorithm over other approaches under several measures.

Keywords: Computer vision; Object detection; Red Palm Weevils; Sparrow search optimization; Deep learning

1. Introduction

One of the harmful insects persisting in palm trees that attack various palm species is the red palm weevil (RPW) [1]. Previously, its presence was considered a medical condition and later caused damage to Africa and northern Europe, east and west sides of Asia, and later spread to the west side of Northern America [2]. The lifetime of weevil species lasts from 45 to 139 days in the palm tree trunk, but it feeds on the palm tissue. It was protected and could not be viewed outside, as the RPW is presented in the tree [3]. Infectious palm trees can live for a long time if there is food, and if the tree seems hollow, the RPW will leave the tree in search of a novel host [4]. It includes four stages throughout its lifetime: adult, egg, pupa, and larva. To control and manage RPWs, first, finding the RPWs is essential. Various methods were devised for providing more precise insect detection outcomes in realtime instead of manual identification approaches [5]. The utility of computer vision (CV) technology through pattern detection has been witnessed as very effective if used to classify and detect insects. There are various benefits to the novel intellectual system, notably, that could be useful for those who lack knowledge to find some insects. Hence, the automatic system would minimize the problem along with the labor effort required to raise the farmer's income. The farmer gets high yield if this is done [6]. Advancements in artificial intelligence (AI) technologies have led to the evolution of automatic systems that present more precise and faster outcomes in pest diagnosis [7]. Nowadays, systems that diagnose wide variety of diseases automatically based on AI are used often. Over the years, several conventional machine learning (ML) approaches are presented

DOI: https://doi.org/10.54216/IJAACI.060202
Received: July 10, 2023 Revised: September 14, 2023 Accepted: November 29, 2023

for the classification and detection of plant diseases [8]. The feature extraction need to do classification in ML is found to be tough and affects the classifier's performance. Increasing speeds and capability of Graphical Processing Unit (GPU) and Central Processing Unit (CPU) led to the progression of novel higher-performance approaches that is process raw data without the necessity of handcrafted features, and this paved way for DL structure [9]. A deep neural network (DNN) structure with several neurons and processing layers can effectively do high-complexity tasks like image recognition and voice by processing large-size datasets [10]. The use of DL approaches methods in the classification and diagnosis of diseases from medical images is common.

This article focuses on the design of automated RPW pest detection using sparrow search optimization with deep learning (RPWPD-SSODL) technique. The RPWPD-SSODL technique employs bilateral filtering (BF) for noise removal process. Next, the RPWPD-SSODL technique uses Dense-RefineDet object detector with ShuffleNet model as a backbone network. For improving the recognition solution, the hyperparameter tuning of the ShuffleNet model can be optimally adjusted by the use of SSO algorithm. To validate the simulation results of the RPWPD-SSODL technique, a comprehensive experimental outcome has been executed.

2. Related Works

Ahmed and Ahmed [11] developed two methods of DL for classifying Palm leaf disease: TL of Inception ResNet and ResNet. The methods help to train hundreds of layers and attain better outcomes. The performance of image classification can be boosted by utilizing ResNet and considering the merit of their potential representation ability. Gibril et al. [12] presented an automated method that depends on a DL method for mapping date palm trees on large scale from very-high-spatial-resolution (VHSR) UAVs dataset. For the semantic segmentations, U-Net (a U-Shape CNN), which depends on a DRL structure, was developed. The performance of the presented method has been compared with different fully convolutional network (FCN) with various encoder structure, which includes two variants of DeepLab V3+, pyramid scene parsing networks and U-Net (depending on VGG16 backbone).

Alburshaid and Mangoud [13] evaluated the ability to use DL in devising a geodatabase in the GIS setting. Two CNN methods were evaluated and presented, the former method uses RetinaNet that applies to the single stage detectors, and the latter method leverages MRCNN that applies to 2-stage detector. Bait-Suwailam [14] presented a numerical electromagnetic method of a low-cost identification modality utilizing resonant-related microwave sensors for detecting RPW pests. Omran [15] intends to find the living phases of RPW that are concealed in palm trees. Nanoparticles and sensors have advantageous adoptions in treatment and detection of date palms. This study portrayed that the RPW infection can be found in the initial stage using Nano-methods. The outcomes of audio analysis are wirelessly informed to control stations to transmit warning messages through the Internet. Delalieux et al. [16] evaluated the potentiality of an RS method for the reliable and timely identification of RPW infestations on the palm canopy. At the same time, detailed optical observation of the RPW effect on palms has been evaluated for assessing the growth of infection from the primary phase till death of palm. A drone-related image processing chain for nondestructive RPW identification has been constructed depending on vegetation and segmentation index analysis methods.

Anis et al. [17] introduced an IoT-related smart palm monitoring model that contribute to the initial identification of RPW infestation 2) utilizing smart agriculture sensors, allowing monitoring palms remotely. Users can utilize mobile application or web to communicate with their palm farmland and support them in obtaining initial identification of infections. To interact among the user as well as sensor layers, the author utilized an industrial-level IoT platform. Parvathy et al. [18] presented a system for initial identification of RPW infections by presenting a portable, smart, non-invasive solution. The system, related to an accelerometer sensor, analyzed signal from palm and check out for specific atrributes in the signals that pest produces. The mechanism produces SMS, audio, and optical warnings for identifying infections.

3. The Proposed Model

In this article, we have mainly focused on designing and developing the RPWPD-SSODL methodology for automated and accurate RPW detection and classification. The presented RPWPD-SSODL system mostly focused on the detection and classification of RPW using computer vision approaches. To accomplish this, the RPWPD-SSODL technique follows a three-phase process: BF-based noise removal, Dense-RefineDet object detector, and SSO-based hyperparameter tuning. Fig. 1 depicts the overall flow of RPWPD-SSODL method.

DOI: https://doi.org/10.54216/IJAACI.060202
Received: July 10, 2023 Revised: September 14, 2023 Accepted: November 29, 2023

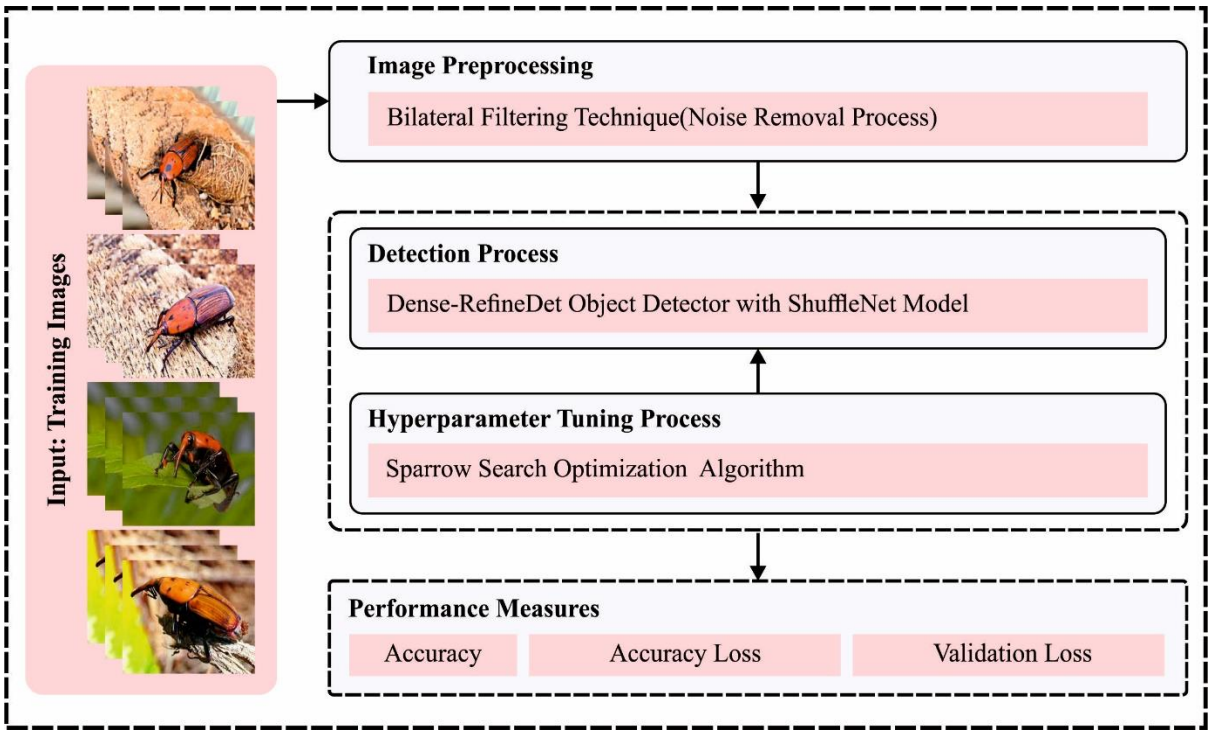

Fig. 1. Overall flow of RPWPD-SSODL method

3.1. Image Pre-processing

To eradicate the noises that exist in the input images, the BF technique is used. The BF is a noise removing process stimulated by the Gaussian filtering (GF) method [19]. While efficiently holding the denoising capability of the GF, it could effectively decrease the additive noise without terminating the details and edges of imagery. The edge data of the imagery can be preserved. However, impulse noise could not be detached. The combinations of two weights define that the conventional BF are grayscale and geometric similarity weights.

$$h(x) = k^{-1}(x)\int_{-\infty}^{\infty}\int_{-\infty}^{\infty} f(\mathfrak{A})c(\mathfrak{A},x)s(f(\mathfrak{A}),f(x)d\mathfrak{A}, \quad (1)$$

Eq. (1), $k(x)$ indicates the normalization index. $c(A,x)$ represents geometric similarity weighted value belonging to central pixel x and its neighboring pixels A, and $s(f(A),f(x))$ shows grayscale similarity weighted of central pixel x and its neighboring pixels A.

$$k(x) = \int_{-\infty}^{\infty}\int_{-\infty}^{\infty} c(\mathfrak{A},x)s\big(f(\mathfrak{A}),f(x)\big)d\mathfrak{A}. \quad (2)$$

The image Gaussian kernel function that defines the geometric similarity can be expressed below

$$c(\mathfrak{A}_X) = \mathrm{e}^{-1/2(d(\mathfrak{A},x)/\sigma_d)}2, \quad (3)$$

In Eq. (3), the central pixel points x and d represent geometric expansion factor, which mostly controls the geometric expansion factors of low-pass filtering strength. $d(A,x)$ shows the distance between neighbouring pixel points A. The small the value of σ_d, the low the low-pass filter strength and the clear the filter outcome:

$$s(f(A),f(x)) = e^{-1/2(f(A)-f(x)/\sigma_r)}2, \quad (4)$$

In Eq. (4), σ_r denotes the diffusion factor of image grayscale similarity. In the classical BF, every pixel should be evaluated more than once, resulting in poor performance. Simultaneously, the parameter is fixed; the parameter must be manually changed as per the actual noise situation.

DOI: https://doi.org/10.54216/IJAACI.060202
Received: July 10, 2023 Revised: September 14, 2023 Accepted: November 29, 2023

3.2. Dense-RefineDet Object Detector

For object detection purposes, the DenseNet-RefineDet model is used. RefineDet refers to a single-stage approach that depends on SSD infrastructure and contains object-detection module (ODM) and anchor-refinement module (ARM) [20]. The ARM allows positive- and negative-refined anchors to ODM to classify and detect goal objects in input imageries. The features in ARM can transport to ODM through an intended transfer connection block (TCB) that accumulates 2 (high-and-low levels) neighboring feature layers in ARM as input and carries out a deconvolution function to high-level layer for attaining features of related size as a low-level layer for making fusion feature with element wise summation. An intended TCB is to offer further contextual data. In this case, it is exploited RefineDet as baseline process for classifying and detecting traffic signs for next reasons: (1) it could be greatly influential owing to its single-stage structure; (2) it exploits a refined approach which simulates a "detection model" to define feasible area in target traffic sign, but its classifications. At this point, our "detection model" varied in typical traffic sign recognition (i.e., recognize every function type particular amongst traffic signs from the original image).

RefineDet can be a great object detection approach utilized for detecting objects with maximum accuracy and speed, but it could not compete with recent approaches at small-object detection. It takes risks because of 2 reasons. Primary, the feature of shallow layers from RefineDet utilized for detecting small objects comprise restricted data that could not be comparatively huge to efficiently small object detection. Multi-scale features can improve outcome from RefineDet, and the shallowest mapping features with maximum resolution can scale at 1/8 the dimension of input images. Because of down-sampling convolutional and pooling functions, data loss takes place, excessive for shallowest resultant layer. The traffic signs of small sized determined in Tsinghua-Tencent 100K database are bounding-box region of <32×3232×32 pixels; thus, the equivalent dimension of smaller traffic sign is <4×44×4 pixels, creating correct detection problem for RefineDet. Secondly, anchors planned utilizing RefineDet could not be appropriate for small object detection, while the centers of every anchor are set at the center of all the cells (0.5, 0.5). It creates it complex for detecting objects of lesser size and placed at junction region of 2 neighboring cells or smaller sized objects beside together.

According to RefineDet approach, dense-refinedet technique is presented by generating a novel Dense-TCB element dependent upon dense connection and integrating an anchor design model. Based on RefineDet, the backbone structure it is choose was VGG-16. It is output 4 distinct scale-feature maps (specially conv7, conv4_3, and conv5_3 layers are chosen for output), and just 2 extra convolutional layers are additional, with second layer utilized for outcome. The Dense-TCB element can execute for transferring extra semantic data in deeper (higher level) feature layer to shallower (lower level) feature layer and specifically for shallowest feature state (conv4_3) for obtaining rich contextual data to detect small-sized traffic signs. A recently planned anchor is utilized for addressing the anchor issue of RefineDet compared to detecting smaller objects.

The RPWPD-SSODL technique uses Dense-RefineDet object detector with ShuffleNet model as a backbone network. A deep network with deep structures keeps great extraction feature ability and usually carries out well from the image tasks [21]. But, the maximum computing and memory necessities of network obstruct wide usage. One method for resolving the problem is to utilize lightweight networks. ShuffleNet is a great lightweight network that decreased computational and parameter costs by the process as channels shuffle from the stage layer. In detail, ShuffleNet comprises convolution, pooling, stage, and fully connected (FC) layers, but the stage contains downsampling and basic units. These units comprise DW convolution layers and 1x1 convolution layers. Nevertheless, ShuffleNet exchanges a vast number of 1x1 point-wise convolutional with channel shuffle, inducing a lack of representative capability and negligible loss of precision. During this stage structure, convolutional optimizer (CO) and cross-stage partial (CSP) structure are implemented to improve the above problem. Eliminating the final convolution layer and replacing the DW convolutional kernel dimensional of 3x3 with 7x7 decreases the model parameter, increases the perceptual domain and gains rich global features. By substituting every DW convolutional 3x3 with 7x7, the padding requires that altered in [1-3]. Thus, the resolution of resultant mapping feature remains similar to the original. The mapping feature of downsampling unit can be divided by the CSP structure into 2 parts, making them pass through distinct paths, and concatenate them composed in the final stage layer. By this function, CSP allows richer gradient set and decreases computation by splits gradient streams for propagating with distinct network paths.

DOI: https://doi.org/10.54216/IJAACI.060202
Received: July 10, 2023 Revised: September 14, 2023 Accepted: November 29, 2023

3.3. Hyperparameter Tuning using SSO Algorithm

To boost the detection performance, the hyperparameter tuning of the ShuffleNet model was conducted using the SSO algorithm. SSO algorithm depends on sparrows' anti-predatory and predatory behaviors in the biological world. Sparrow is generally separated into followers and producers to complete the foraging [22]. In their natural state, sparrows observe one another. While foraging, each sparrow keeps alert to the nearby environments to avoid arrival of natural enemies:

$$X = \begin{bmatrix} x_{1,1} & x_{1,2} & \cdots & x_{1,\mathrm{d}} \\ x_{2,1} & x_{2,2} & \cdots & x_{2,\mathrm{d}} \\ \vdots & \vdots & \vdots & \vdots \\ x_{n_p,1} & x_{n_p,2} & \cdots & x_{n_p,\mathrm{d}} \end{bmatrix} \tag{5}$$

In Eq. (5), n_p denotes the amount of sparrows, and d indicates the dimension of variable:

$$F_x = \begin{bmatrix} f([x_{1,1} & x_{1,2} & \cdots & x_{1,\mathrm{d}}]) \\ f([x_{2,1} & x_{2,2} & \cdots & x_{2,\mathrm{d}}]) \\ & \vdots & & \\ f([x_{n_p,1} & x_{n_p,2} & \cdots & x_{n_p,\mathrm{d}}]) \end{bmatrix} \tag{6}$$

In Eq. (6), the values of every line in F_x show sparrows' fitness value.

In SSO algorithm, the producers usually contain more enormous energy reserves. They are accountable to search the whole population for areas with rich food, which provides each participant with the area of foraging and direction. Sparrow fitness values define energy reserves. individuals with high fitness value have the highest preference in attaining food, which drives the whole population to find food as producer:

$$X_{i,j}^{t+1} = \begin{cases} X_{i,j}^{t} \cdot \exp\left(\dfrac{-i}{\alpha \cdot iter_{\max}}\right) & R_2 < ST \\ X_{i,j}^{t} + Q \cdot L & R_2 \geq ST \end{cases} \tag{7}$$

In Eq. (7), t symbolizes the amount of existing iterations, $j = (1,2,\ldots,d)$, Q denotes a normal distribution random value subjected to [0,1]. $X_{i,j}^{t}$ shows the $j\text{-}th$ dimension location of the i^{th} sparrow at t iteration. $iter_{\max}$ depicts the maximal amount of iterations. α denotes the randomly generated value (0,1), $R_2 \in [0,1]$ and $ST \in [0.5,1]$, R_2 and ST indicate warning values and safety values, correspondingly. L denotes the matrix of $1 \times d$, and every competent inside is 1. Where $R_2 \geq ST$, it implies that sparrow has found natural enemy, and each sparrow needs to quickly fly to other safer regions. If $R_2 < ST$, it implies that not any natural enemy around, and producer conducted a comprehensive search mode.

The follower is a type of sparrow with poor fitness value and lower energy in the population:

$$X_{i,j}^{t+1} = \begin{cases} Q \cdot \exp\left(\dfrac{x_{worst}^{t} - x_{i,i}^{t}}{i^2}\right) & i > \dfrac{n_p}{2} \\ X_p^{t+1} + |X_{i,j}^{t} - X_p^{t+1}| \cdot A^{+} \cdot L & other \end{cases} \tag{8}$$

In Eq. (8), X_P shows the better location for producer, X_{worst} indicates the worst place, A denotes the matrix of $1 \times d$, all the components in matrix can be alloted randomly with the value of 1 or -1, $A^{+} = A^{T}(AA^{T})^{-1}$. If $I > n_p/2$, it implies that i^{th} followers with worse fitness value don't obtain food and is in state of hunger. Now, it should fly to other locations for food to attain greater energy

Simultaneously, the sparrow population has early warning and detection behavior: While finding food, few sparrows serve as a scout, which alerts others. Once the danger occurs, they abandon the present food source. Whether the follower or producer would present food and take new role. SD sparrows are selected randomly from the population for earlier warning behavior:

DOI: https://doi.org/10.54216/IJAACI.060202
Received: July 10, 2023 Revised: September 14, 2023 Accepted: November 29, 2023

$$X_{i,j}^{t+1} = \begin{cases} X_{best}^{t} + \overline{\beta} \cdot |X_{i,j}^{t} - X_{best}^{t}| \; f_i > f_g \\ X_{i,j}^{t} + K \cdot \left(\frac{|X_{i,i}^{t} - X_{worst}^{t}|}{(f_i - f_w) + \varepsilon} \right) f_i = f_g \end{cases} \quad (9)$$

In Eq. (9), $K \in [-1,1]$ denotes the uniform random integer. X_{best} denotes the global optimum location, f_i shows the fitness value of the existing sparrow. $\overline{\beta}$ shows the step control parameter, a normal distribution random integer within [0,1], $f_{g}{}^{and}h$ represents the present global best and poor fitness values, correspondingly. ε shows the minimal constant to prevent a 0 in denominator. $f_i = f_g$ shows that sparrows within the middle of population are aware of hazard; hence it must be closer to other individuals. If $f_i > f_g$, it implies that sparrow is at the population edge and are highly vulnerable to natural enemy. K can be a step control parameter and denotes the direction of movement of sparrow.

The SSO approach grows a fitness function (FF) to realize higher classifier performances. It expresses a positive integer that indicated the best solution for candidate outcomes. During this case, the decreasing classifier errors have been supposed to be FF, as defined in Eq. (10).

$$fitness(x_i) = ClassifierErrorRate(x_i)$$

$$= \frac{No.of\ misclassified\ instances}{Total\ no.of\ instances} * 100 \quad (10)$$

4. Results Analysis

In the section, the RPW detection outcome of the RPWPD-SSODL algorithm are studied on the dataset comprising different RPW images [23, 24]. Fig. 2 illustrates the sample images. Fig. 3 demonstrates the original and detection images.

Fig. 2. Sample Images

DOI: https://doi.org/10.54216/IJAACI.060202
Received: July 10, 2023 Revised: September 14, 2023 Accepted: November 29, 2023

Fig. 3. a) Original Images b) Detection Images

Table 1 and Fig. 4 represented the entire RPW recognition results of the RPWPD-SSODL system at various epochs. The experimental outcomes reported that the RPWPD-SSODL methodology achieved enhanced results under all epochs. For sample, on image-1, the RPWPD-SSODL technique attains $accu_y$ of 99.72%, 99.74%, 99.40%, 99.18%, 99.88%, and 99.78% under 500, 1000, 1500, 2000, 2500, and 3000 epochs. Simultaneously, on image-4, the RPWPD-SSODL method attains $accu_y$ of 99.83%, 99.98%, 99.51%, 99.85%, 99.19%, and 99.71% under 500, 1000, 1500, 2000, 2500, and 3000 epochs. Meanwhile, on image-6, the RPWPD-SSODL approach attains $accu_y$ of 99.79%, 99.43%, 99.82%, 99.82%, 99.33%, and 99.11% under 500, 1000, 1500, 2000, 2500, and 3000 epochs. Moreover, on image-8, the RPWPD-SSODL algorithm attains $accu_y$ of 99.50%, 99.85%, 99.28%, 99.70%, 99.60%, and 99.76% under 500, 1000, 1500, 2000, 2500, and 3000 epochs. Furthermore, on image-10, the RPWPD-SSODL approach attains $accu_y$ of 99.86%, 99.06%, 99.68%, 99.52%, 99.14%, and 99.42% under 500, 1000, 1500, 2000, 2500, and 3000 epochs.

Fig. 5 depicts an average RPW detection result of the RPWPD-SSODL system under various epochs. The outcome highlighted that the RPWPD-SSODL system reaches effectual outcomes under each epoch. It is observed that the RPWPD-SSODL technique offers average $accu_y$ of 99.62%, 99.53%, 99.58%, 99.60%, 99.48%, and 99.58% under 500, 1000, 1500, 2000, 2500, and 3000 epochs.

Table 1: RPW recognition outcome of RPWPD-SSODL approach with distinct epochs and test images

Test Images	Epoch500	Epoch1000	Epoch1500	Epoch2000	Epoch2500	Epoch3000
Image-1	99.72	99.74	99.40	99.18	99.88	99.78
Image-2	99.83	99.44	99.93	99.35	99.57	99.17
Image-3	99.27	99.07	99.90	99.72	99.71	99.04
Image-4	99.83	99.98	99.51	99.85	99.19	99.71
Image-5	99.59	99.81	99.06	99.97	99.57	99.88
Image-6	99.79	99.43	99.82	99.82	99.33	99.11

DOI: https://doi.org/10.54216/IJAACI.060202
Received: July 10, 2023 Revised: September 14, 2023 Accepted: November 29, 2023

Image-7	99.10	99.61	99.94	99.16	99.50	99.90
Image-8	99.50	99.85	99.28	99.70	99.60	99.76
Image-9	99.68	99.29	99.24	99.70	99.32	99.99
Image-10	99.86	99.06	99.68	99.52	99.14	99.42
Average	**99.62**	**99.53**	**99.58**	**99.60**	**99.48**	**99.58**

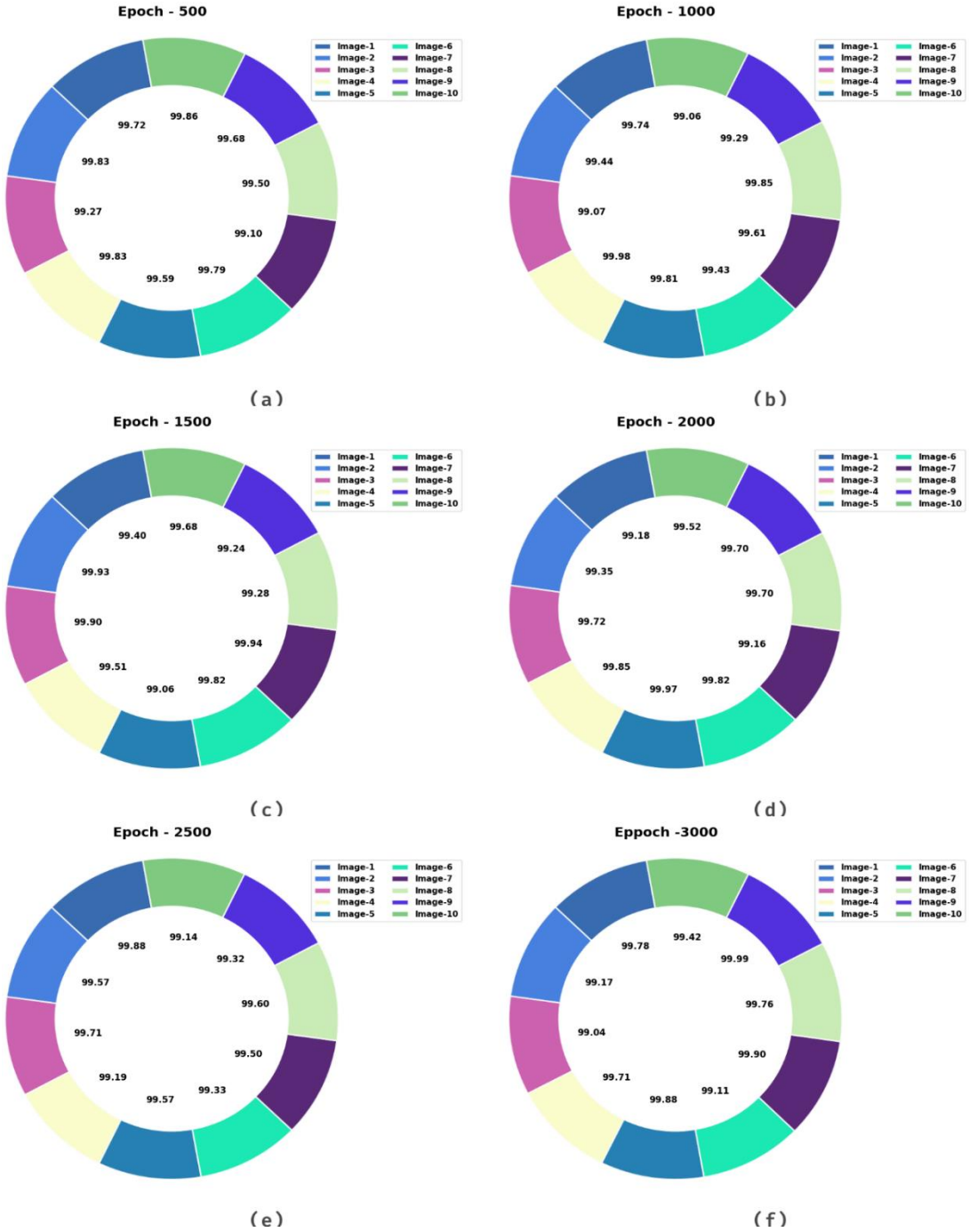

Fig. 4. RPW detection outcome of RPWPD-SSODL system (a-f) Epochs 500-3000

DOI: https://doi.org/10.54216/IJAACI.060202
Received: July 10, 2023 Revised: September 14, 2023 Accepted: November 29, 2023

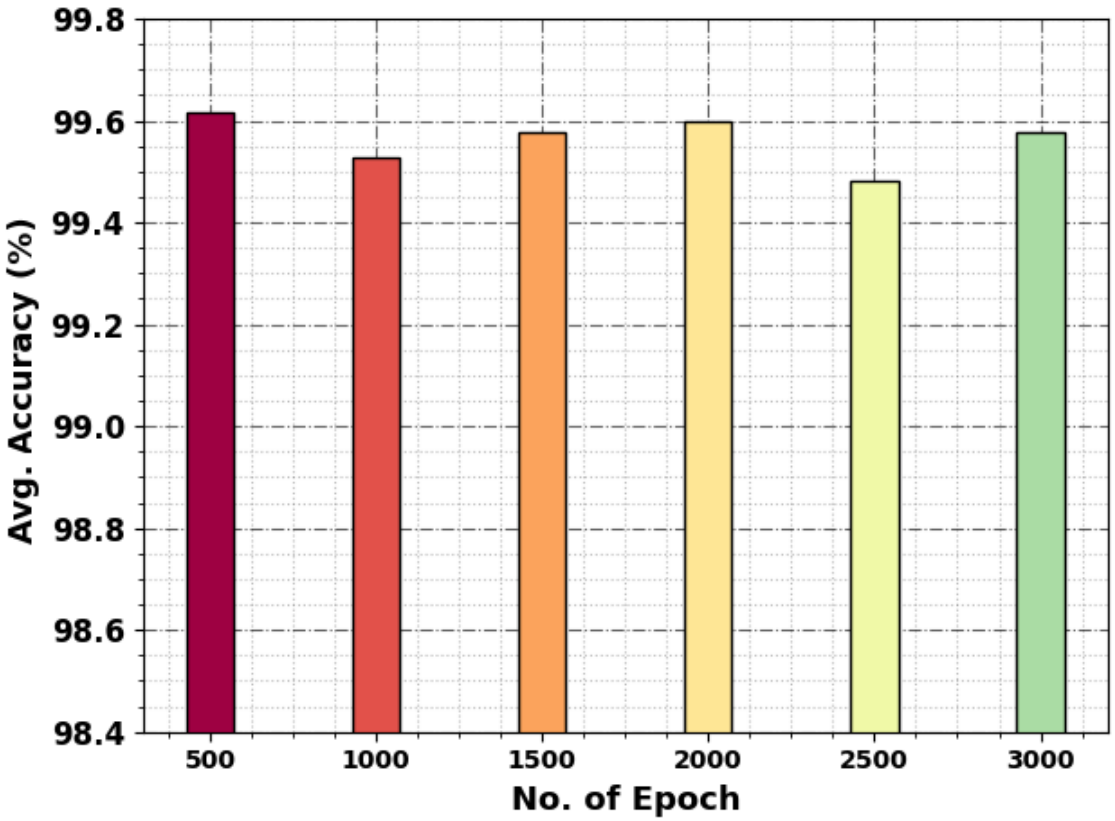

Fig. 5. Average of RPWPD-SSODL approach with distinct epochs

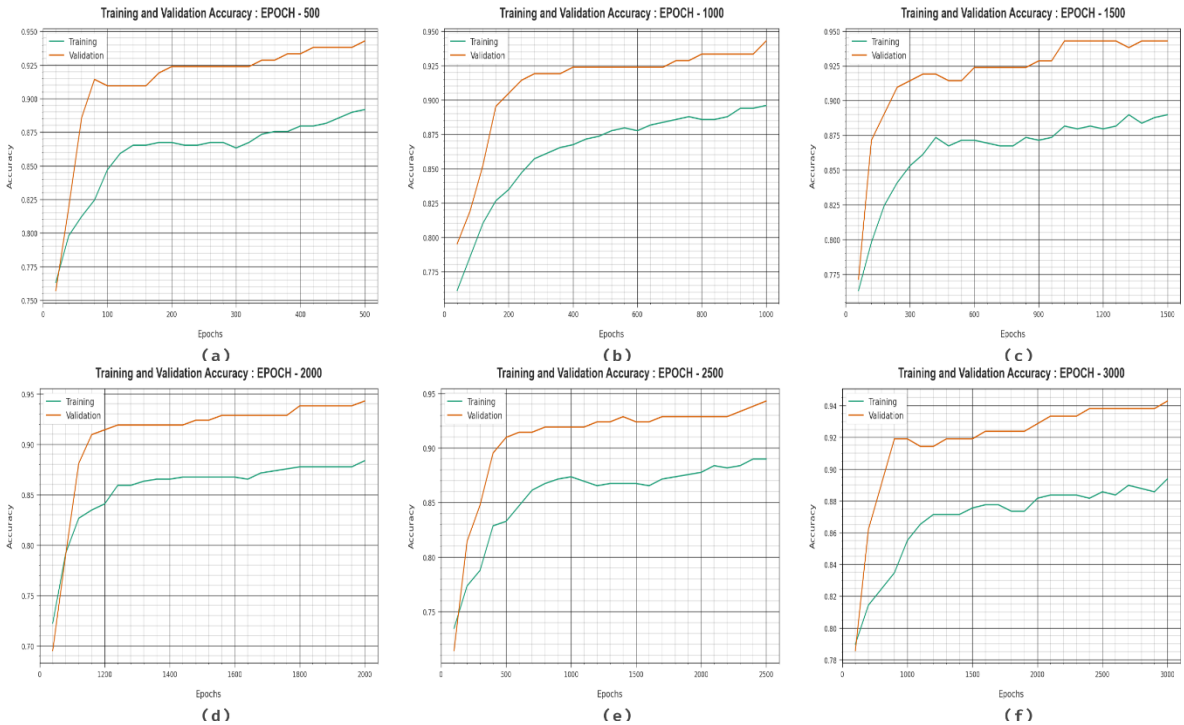

Fig. 6. Accuracy curve of RPWPD-SSODL approach (a-f) Epoch 500-3000

DOI: https://doi.org/10.54216/IJAACI.060202
Received: July 10, 2023 Revised: September 14, 2023 Accepted: November 29, 2023

Fig. 6 inspects the RPWPD-SSODL approach's accuracy in training and validation on various epochs. The outcomes specified that the RPWPD-SSODL methodology has higher $accu_y$ values with maximum epochs. Moreover, the enhancing $accu_y$ with training $accu_y$ pointed out that the RPWPD-SSODL method attains productively on distinct epochs.

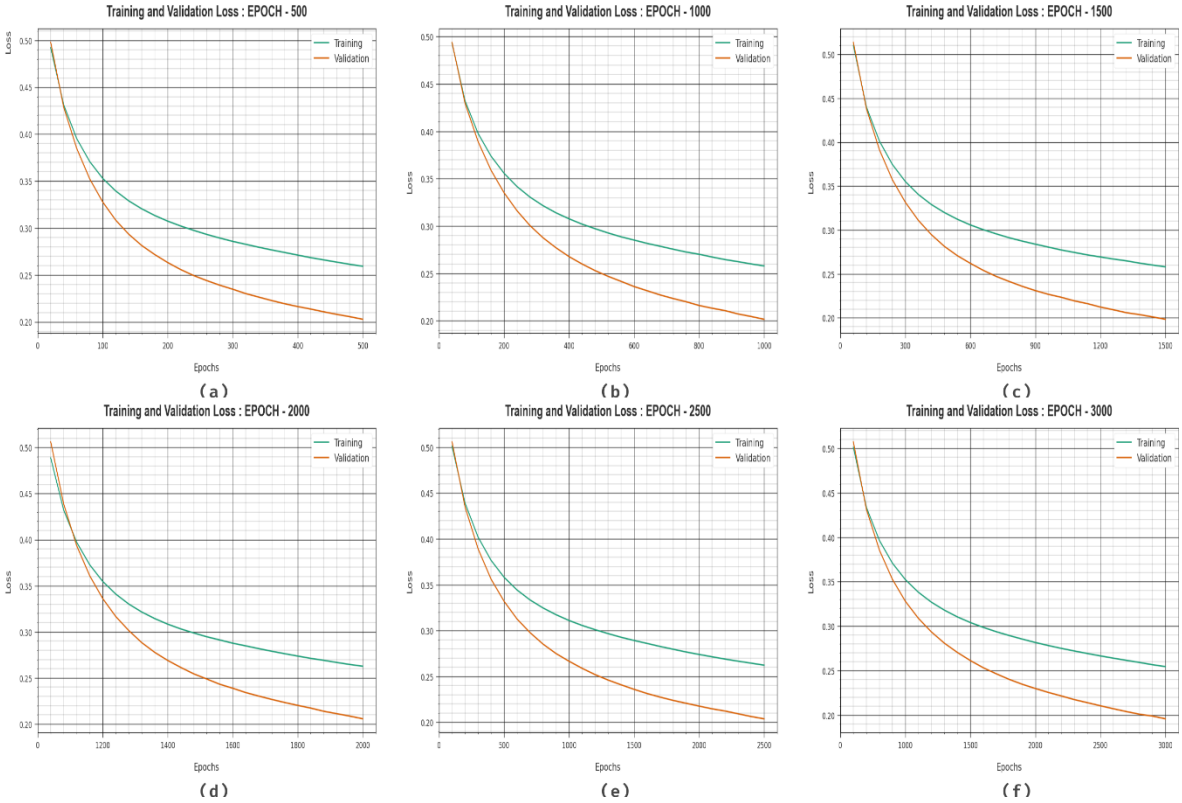

Fig. 7. Loss curve of RPWPD-SSODL methodology (a-f) Epochs 500-3000

The loss curve of the RPWPD-SSODL approach in training and validation is given on different epochs in Fig. 7. The figure indicates that the RPWPD-SSODL algorithm attained nearer performances of training and validation losses. The RPWPD-SSODL method gains capably on distinct epochs.

Table 2: $Accu_y$ analysis of RPWPD-SSODL algorithm with recent algorithms

Methods	**Accuracy (%)**
SVM	93.11
NB	82.60
RF	93.09
MLP	93.07
AdaBoost	93.10
Faster RCNN	99.03
RPWPD-SSODL	99.62

Finally, a detailed $accu_y$ investigation of the RPWPD-SSODL technique with recent approaches is in Table 2 and Fig. 8 [2]. The simulation values represented the poor performance of the SVM model with least $accu_y$ of 82.60%. The other recent approaches, such as SVM, RF, MLP, and AdaBoost approaches have obtained reasonably closer performance. But the RPWPD-SSODL technique shows promising performance with maximum $accu_y$ of 99.62%. These outcomes highlighted the optimum performance of the RPWPD-SSODL technique with other recent models.

DOI: https://doi.org/10.54216/IJAACI.060202
Received: July 10, 2023 Revised: September 14, 2023 Accepted: November 29, 2023

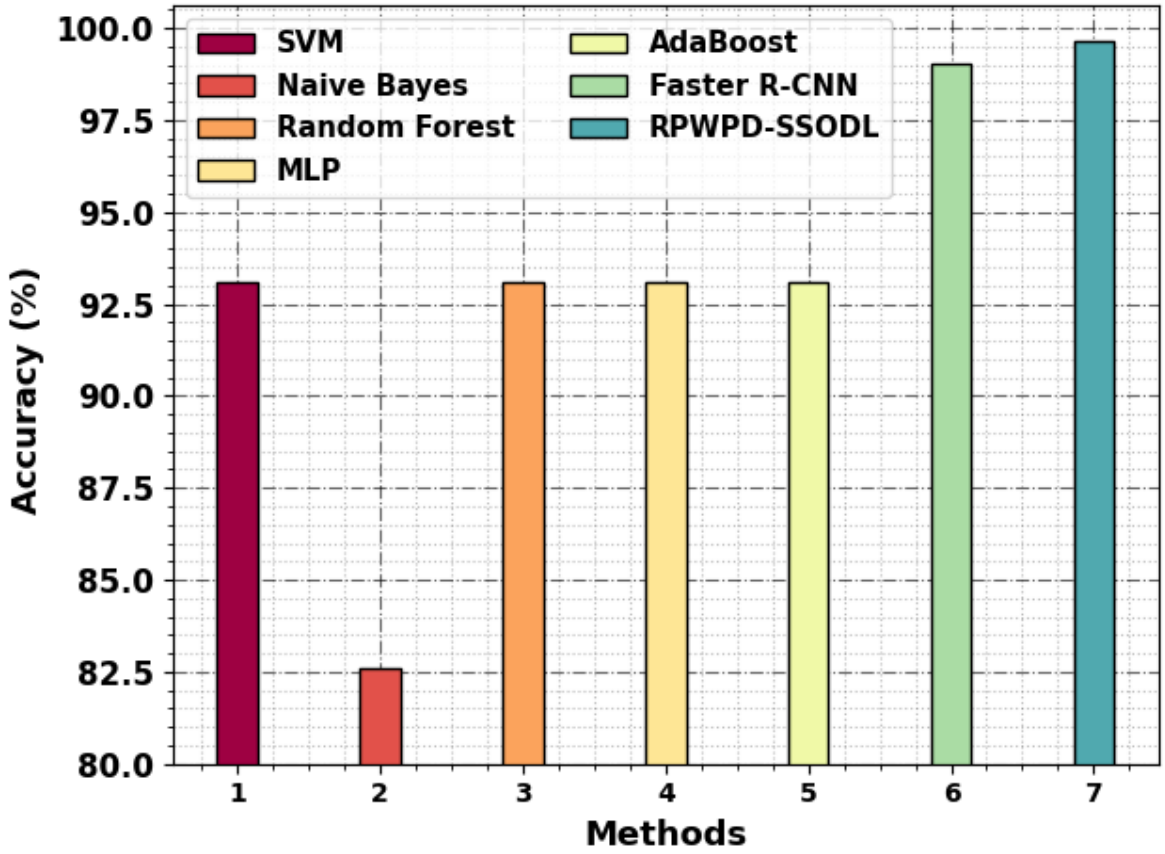

Fig. 8. $Accu_y$ analysis of RPWPD-SSODL approach with recent algorithms

5. Conclusion

In this article, we have mainly focused on designing and developing the RPWPD-SSODL algorithm for automated and accurate RPW detection and classification. The presented RPWPD-SSODL technique mainly focused on identifying and classifying RPW using computer vision approaches. To accomplish this, the RPWPD-SSODL technique follows a three-phase process: BF based noise removal, Dense-RefineDet object detector, and SSO based hyperparameter tuning. The RPWPD-SSODL technique uses Dense-RefineDet object detector with ShuffleNet model as a backbone network. For improving the detection performance, the hyperparameter tuning of the ShuffleNet model can be optimally adjusted by the use of SSO algorithm. To validate the simulation results of the RPWPD-SSODL technique, a comprehensive simulation analysis can be implemented. The simulation outcome highlighted the betterment of the RPWPD-SSODL technique over other existing algorithms under several measures. In future, weighted voting ensemble classifier has been designed to improve the overall RPW classification solution.

References

[1] Manee, M.M., Alqahtani, F.H., Al-Shomrani, B.M., El-Shafie, H.A. and Dias, G.B., 2023. Omics in the Red Palm Weevil Rhynchophorus ferrugineus (Olivier)(Coleoptera: Curculionidae): A Bridge to the Pest. *Insects*, *14*(3), p.255.

[2] Alsanea, M., Habib, S., Khan, N.F., Alsharekh, M.F., Islam, M. and Khan, S., 2022. A Deep-Learning Model for Real-Time Red Palm Weevil Detection and Localization. *Journal of Imaging*, *8*(6), p.170.

[3] Eldin, H.A., Waleed, K., Samir, M., Tarek, M., Sobeah, H. and Salam, M.A., 2020, November. A Survey on Detection of Red Palm Weevil Inside Palm Trees: Challenges and Applications. In *Proceedings of the 2020 9th International Conference on Software and Information Engineering (ICSIE)* (pp. 119-125).

DOI: https://doi.org/10.54216/IJAACI.060202
Received: July 10, 2023 Revised: September 14, 2023 Accepted: November 29, 2023

[4] Kurdi, H., Al-Aldawsari, A., Al-Turaiki, I. and Aldawood, A.S., 2021. Early detection of red palm weevil, Rhynchophorus ferrugineus (Olivier), infestation using data mining. *Plants*, *10*(1), p.95.

[5] Ashry, I., Wang, B., Mao, Y., Sait, M., Guo, Y., Al-Fehaid, Y., Al-Shawaf, A., Ng, T.K. and Ooi, B.S., 2022. CNN–Aided Optical Fiber Distributed Acoustic Sensing for Early Detection of Red Palm Weevil: A Field Experiment. *Sensors*, *22*(17), p.6491.

[6] Al-Shalout, M. and Mansour, K., 2021, December. Detecting date palm diseases using convolutional neural networks. In *2021 22nd International Arab Conference on Information Technology (ACIT)* (pp. 1-5). IEEE.

[7] Habineza, P., Muhammad, A., Ji, T., Xiao, R., Yin, X., Hou, Y. and Shi, Z., 2019. The promoting effect of gut microbiota on growth and development of red palm weevil, Rhynchophorus ferrugineus (Olivier)(Coleoptera: Dryophthoridae) by modulating its nutritional metabolism. *Frontiers in microbiology*, *10*, p.1212.

[8] Karar, M.E., Abdel-Aty, A.H., Algarni, F., Hassan, M.F., Abdou, M.A. and Reyad, O., 2022. Smart IoT-based system for detecting RPW larvae in date palms using mixed depthwise convolutional networks. *Alexandria Engineering Journal*, *61*(7), pp.5309-5319.

[9] Hajjaji, Y., Boulila, W. and Farah, I.R., 2022. Leveraging Artificial Intelligence Techniques for Smart Palm Tree Detection: A Decade Systematic Review. *Procedia Computer Science*, *207*, pp.2823-2832.

[10] Alburshaid, E.A. and Mangoud, M.A., 2021, December. Developing Date Palm Tree Inventory from Satellite Remote Sensed Imagery using Deep Learning. In *2021 3rd IEEE Middle East and North Africa COMMunications Conference (MENACOMM)* (pp. 54-59). IEEE.

[11] Ahmed, M. and Ahmed, A., 2023. Palm tree disease detection and classification using residual network and transfer learning of inception ResNet. *Plos one*, *18*(3), p.e0282250.

[12] Gibril, M.B.A., Shafri, H.Z.M., Shanableh, A., Al-Ruzouq, R., Wayayok, A. and Hashim, S.J., 2021. Deep convolutional neural network for large-scale date palm tree mapping from UAV-based images. *Remote Sensing*, *13*(14), p.2787.

[13] Alburshaid, E.A. and Mangoud, M.A., 2021, October. Palm Trees Detection Using the Integration between GIS and Deep Learning. In *2021 International Symposium on Networks, Computers and Communications (ISNCC)* (pp. 1-6). IEEE.

[14] Bait-Suwailam, M.M., 2021. Numerical assessment of red palm weevil detection mechanism in palm trees using CSRR microwave sensors. *Progress In Electromagnetics Research Letters*, *100*, pp.63-71.

[15] Omran, E.S.E., 2020. Nano-technology for real-time control of the red palm weevil under climate change. *Climate Change Impacts on Agriculture and Food Security in Egypt: Land and Water Resources—Smart Farming—Livestock, Fishery, and Aquaculture*, pp.321-344.

[16] Delalieux, S., Hardy, T., Ferry, M., Gomez, S., Kooistra, L., Culman, M. and Tits, L., 2023. Red Palm Weevil Detection in Date Palm Using Temporal UAV Imagery. *Remote Sensing*, *15*(5), p.1380.

[17] Anis, K., Abdulrahman, A., Bassel, S., Abdullatif, H., Mohanned, A., Abdulrahman, S., Hesham, A., Adel, A. and Mohamed, A., 2020. Smart palm: an IoT framework for red palm weevil early detection. *Agronomy*, *10*(7).

[18] Parvathy, S.R., Pathrose, N., Rajesh, K.R., Varghese, J., Vishnu, S., Mathew, N. and Kallara, S.B., 2022, August. Red Palm Weevil Detection System for Early Warning and Mitigation of Crop Loss. In *2022 International Conference on Connected Systems & Intelligence (CSI)* (pp. 1-5). IEEE.

[19] Charchekhandra, B. (2023). Align and fusion two thermal and visual images. *Pure Mathematics for Theoretical Computer Science*, 1(1), 17-31.

[20] Li, H. and Duan, X.L., 2022. SAR Ship Image Speckle Noise Suppression Algorithm Based on Adaptive Bilateral Filter. *Wireless Communications and Mobile Computing*, *2022*.

[21] Sun, C., Ai, Y., Wang, S. and Zhang, W., 2020. Dense-RefineDet for traffic sign detection and classification. *Sensors*, *20*(22), p.6570.

[22] Zheng, L., Zhao, M., Zhu, J., Huang, L., Zhao, J., Liang, D. and Zhang, D., 2022. Fusion of hyperspectral imaging (HSI) and RGB for identification of soybean kernel damages using ShuffleNet with convolutional optimization and cross stage partial architecture. Frontiers in Plant Science, 13.

[23] Liu, H., Dai, J. and Chen, X., 2023. A Moving Window Double Locally Weighted Extreme Learning Machine on an Improved Sparrow Searching Algorithm and Its Case Study on a Hematite Grinding Process. *Processes*, *11*(1), p.169.

[24] Atassi, Layal; El-Shamaa, Khaled; Biradar, Chandrashekhar, 2019, "Al_Khattem Potential Hot-spots Of Red Palm Weevil (RPW) Risk Based On Trap-data 2016", https://hdl.handle.net/20.500.11766.1/FK2/EY1UHA, MELDATA, V3.

[25] https://data.mel.cgiar.org/dataset.xhtml?persistentId=hdl:20.500.11766.1/FK2/EY1UHA&version=3.0&selectTab=termsTab

DOI: https://doi.org/10.54216/IJAACI.060202
Received: July 10, 2023 Revised: September 14, 2023 Accepted: November 29, 2023